

Krzysztof WIERZCHOLSKI*, **Andrzej MISZCZAK****,
Andrei KHUDDOLEY***

MEASUREMENT OF UNUSED MICROBEARING GROOVED SURFACES FOR COMPUTER VENTILATOR

POMIAR NIEUŻYWANYCH POWIERZCHNI MIKROŁOŻYSK Z NANORÓWKAMI WENTYLATORA KOMPUTEROWEGO

Key words:

computer ventilator, microbearing, herringbone grooves, nano-profiles, surfaces

Słowa kluczowe:

wentylator komputerowy, mikrołożyska, rowki w jodełkę, nanoprofile, powierzchnie

* Koszalin University of Technology, Institute of Mechatronics, Nanotechnology and Vacuum Technique, PL 75-453 Koszalin, ul. Śniadeckich 2, Poland; krzysztof.wierzcholski@wp.pl.

** Maritime University Gdynia, Morska Street 81-87, 81-225 Gdynia, Poland; miszczak@am.gdynia.pl.

*** Luikov Heat and Mass Transfer Institute of National Academy of Sciences of Belarus, Minsk, khudoley@yahoo.com.

Summary

This paper presents a measurement analysis of two, new, non-damaged cooperating micro-bearing surfaces occurring in computer ventilator Kama Flow SP0825FDB12H 0.080 m. Such surfaces are radically different in comparison with surfaces that are found in HDD microbearings. Developed measurements concern Scanning Electron Microscope (SEM), Mira TESCAN INCA, and illustrate 350 images of journal and sleeve work surfaces using the Microscopy system. This paper also concerns roughness tests with 3D images of journal and sleeve work surfaces and profiles of their cross sections utilising Atomic Force Microscopy (AFM), NT-206, Microtestmachines Ltd, Belarus. Vickers micro-hardness value studies for journal and sleeve surface are performed too. Research studies of the sleeve surface included measurements for macro-profile surfaces with herringbone grooves and AFM micro-profiles of small grooves. The measurements are performed for a new undamaged journal and sleeve surface utilising the Atomic Force Microscope and SEM & Micro-X-Ray analysis. Such analysis concern results referring to the bearing material composition with standard deviation of measured values.

INTRODUCTION

The flow of the lubricant in cylindrical micro-bearing gap is generated by the rotation of the journal with the angular velocity ω and rotational speed 2900 rpm with oil viscosity 0.018 Pas [L. 1]. A slide microbearing has been recently used in a computer ventilator replacing the conventional ball bearings, due to its outstanding low noise and vibration characteristics [L. 2, 4]. In this application, herringbone grooves have the advantage of self-sealing, which causes the lubricant to be pumped inward, and therefore, reduces side leakage. They also prevent whirl instability that is observed in the plain journal bearings at concentric operating conditions [L. 1, 3, 5, 6]. Groove location has an influence on the dynamic performances in computer ventilator microbearing. Fig. 1 shows the microbearing with various grooves in journal and sleeve [L. 3].

The diameter of the journal is 0.003 m, radial clearance $3.15 \cdot 10^{-6}$ m, groove angle 26° , and the groove type is herringbone. Symmetric grooves of the journal microbearing generate the concentric motion of a rotor at the origin, but asymmetric grooves generate the concentric rotation with the eccentricity ratio of 0.2. The measured sample concerning the journal and sleeve in a new undamaged micro-bearing surfaces is presented in Fig. 2.

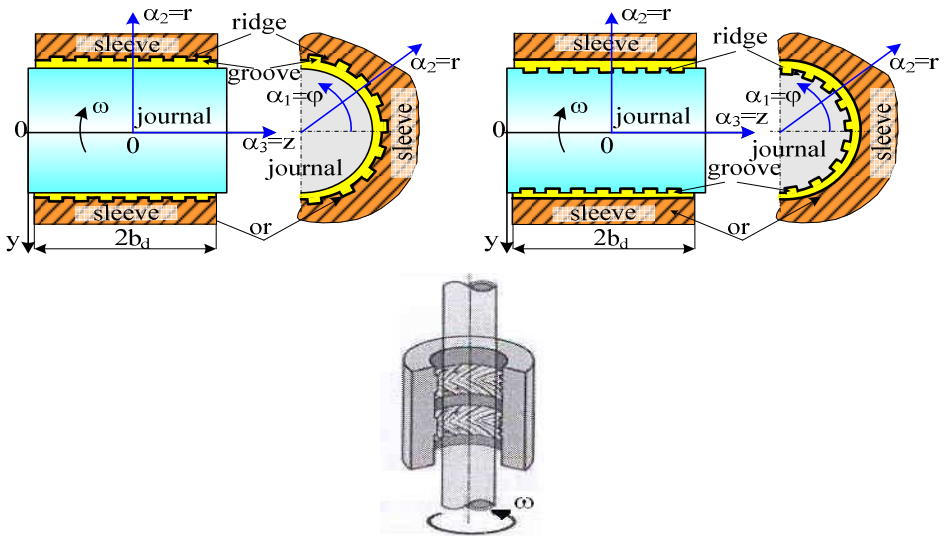


Fig. 1. The view of cylindrical microbearing journal surfaces with nano-ridges and grooves

Rys. 1. Widok powierzchni walcowego mikrołożyska ślizgowego z nanozęberkami

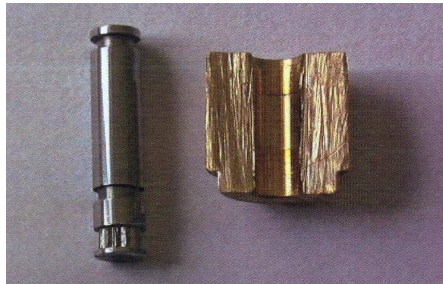


Fig. 2. The view of measured unused and undamaged surfaces with nano-ridges and grooves in cylindrical slide microbearing journal and sleeve, for computer ventilator Kama Flow SP0825FDB12H

Rys. 2. Widok nowych, nieużytych, nieuszkodzonych powierzchni czopa i panewki z nanozęberkami i rowkami w cylindrycznym mikrołożysku ślizgowym komputerowego wentylatora Kama Flow SP0825FDB12H

SEM & MICRO X-RAY ANALYSIS OF THE JOURNAL WORK SURFACE

The journal is made from Steel X20 Cr13 EN10250-4. The bearing material consists of the following: silicium (Si), chromium (Cr), manganese (Mn), and iron (Fe). Percentage values of the mentioned ingredients are given in **Table 1**.

The values are measured three times for three spectrum. The standard deviation values of measured results are calculated.

Fig. 3 illustrates the image of the journal work surface in two enlarged scales, using the Digital Microscopy Imaging. **Fig. 3a** presents the surface $86.80\ \mu\text{m} \times 86.80\ \mu\text{m}$ and the enlarged picture is shown in **Fig. 3b** and describes the region enlarged (10x), namely, $8.680\ \mu\text{m} \times 8.680\ \mu\text{m}$. On the journal surface, the grooves do not occur. There are a lot of scratches on surface (**Fig. 3a**) smaller than $1\ \mu\text{m}$ wide. **Fig. 3b** shows the shape (morphology) and small porosity of the surface.

Table 1. X-Ray analysis results of percent values of ingredients occurring in journal bearing material

Tabela 1. Procentowe wartości składników występujących w materiale czopa uzyskane metodą analizy rentgenowskiej

Ingredients	Si	Cr	Mn	Fe	Total
Spectrum 1	0.80	13.72	0.54	84.94	100.00
Spectrum 2	0.92	13.47	0.63	84.99	100.00
Spectrum 3	0.92	13.53	0.48	85.07	100.00
Average	0.88	13.57	0.55	85.00	100.00
Standard deviation	0.07	0.13	0.07	0.06	
Maximum value	0.92	13.72	0.63	85.07	
Minimum value	0.80	13.47	0.48	84.94	

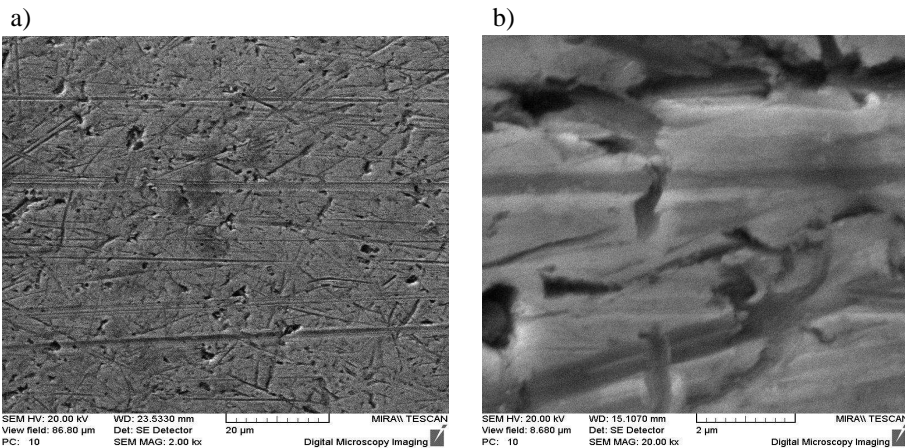


Fig. 3. SEM – image of work surface of microbearing journal in computer ventilator Kama Flow: a) view field $86.80\ \mu\text{m} \times 86.80\ \mu\text{m}$, b) view field: $8.680\ \mu\text{m} \times 8.680\ \mu\text{m}$

Rys. 3. SEM – obrazy powierzchni roboczej czopa w mikrołożysku wentylatora komputerowe-
go Kama Flow: a) widok pola $86,80\ \mu\text{m} \times 86,80\ \mu\text{m}$, b) widok pola: $8,680\ \mu\text{m} \times 8,680\ \mu\text{m}$

SEM & MICRO X-RAY ANALYSIS OF THE SLEEVE WORK SURFACE

The sleeve is made from brass alloy CB763S EN 1982. The alloy consists of the following: copper (Cu), and zinc (Zn). Percentage values of the mentioned ingredients are given in **Table 2**. The values are measured only once for one spectrum.

Table 2. X-Ray analysis results of percent values of ingredients occurring in the alloy on the sleeve work surface

Tabela 2. Procentowe wartości składników występujących w materiale panewki uzyskane metodą analizy rentgenowskiej

Ingredients	Cu	Zn	Total
Spectrum 1	60.23	39.77	100.00
Average	60.23	39.77	100.00
Standard deviation	0.00	0.00	
Maximum value	60.23	39.77	
Minimum value	60.23	39.77	

Fig. 4 illustrates the image of the sleeve work surface in three successive enlarged scales, using the Digital Microscopy Imaging. **Fig. 4a** presents the surface $1740 \cdot 10^{-6} \text{ m} \times 1740 \cdot 10^{-6} \text{ m}$, and the enlarged pictures showed in **Figs. 4b** and **4c** describe the regions $86.8 \cdot 10^{-6} \text{ m} \times 86.8 \cdot 10^{-6} \text{ m}$, $300 \cdot 10^{-6} \text{ m} \times 480 \cdot 10^{-6} \text{ m}$, respectively.

The sleeve surface has herringbone and longitudinal grooves. **Fig. 4a** illustrates the herringbone grooves. Enlargement view field ($300 \cdot 10^{-6} \text{ m} \times 480 \cdot 10^{-6} \text{ m}$) in **Fig. 4c** illustrates the herringbone groove and smaller regular longitudinal grooves. The highest enlargement field $86.8 \cdot 10^{-6} \text{ m} \times 86.8 \cdot 10^{-6} \text{ m}$ presented in **Fig. 4b** shows only the regular longitudinal grooves. Longitudinal and herringbone grooves are from 10 to $50 \cdot 10^{-9} \text{ m}$ wide.

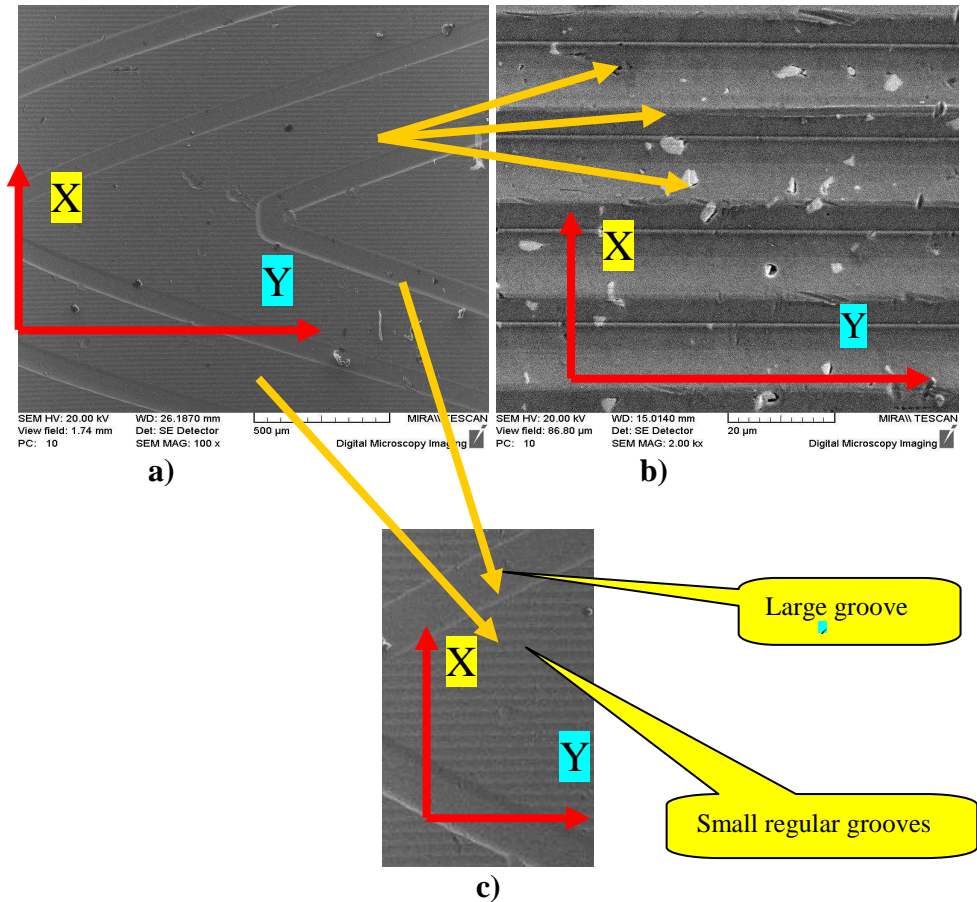


Fig. 4. SEM – image of work surface of the sleeve: a) view field: $1740 \cdot 10^{-6} \text{ m} \times 1740 \cdot 10^{-6} \text{ m}$, b) view field: $86.8 \cdot 10^{-6} \text{ m} \times 86.8 \cdot 10^{-6} \text{ m}$, c) view field: $300 \cdot 10^{-6} \text{ m} \times 480 \cdot 10^{-6} \text{ m}$

Rys. 4. SEM – obrazy powierzchni roboczej panewki: a) widok pola $1740 \cdot 10^{-6} \text{ m} \times 1740 \cdot 10^{-6} \text{ m}$, widok pola: $86.8 \cdot 10^{-6} \text{ m} \times 86.8 \cdot 10^{-6} \text{ m}$, c) widok pola: $300 \cdot 10^{-6} \text{ m} \times 480 \cdot 10^{-6} \text{ m}$

AFM ROUGHNESS TEST FOR JOURNAL SURFACE

Roughness of the journal working surface is measured in 3D space by the Atomic Force Microscope NT-206 with silicon cantilever CSC38 with $10 \cdot 10^{-9} \text{ m}$ tip radius. We have shown the view field $20500 \text{ nm} \times 20100 \text{ nm} \times 384.9 \text{ nm}$ and have calculated the average roughness $R_a = 21.4 \text{ nm}$, and the root mean square $R_q = 28.6 \text{ nm}$. The results are presented in **Fig. 5**.

The cross section along the sample presented in **Fig. 5** illustrates the height roughness and profile of the journal surface in **Fig. 6**.

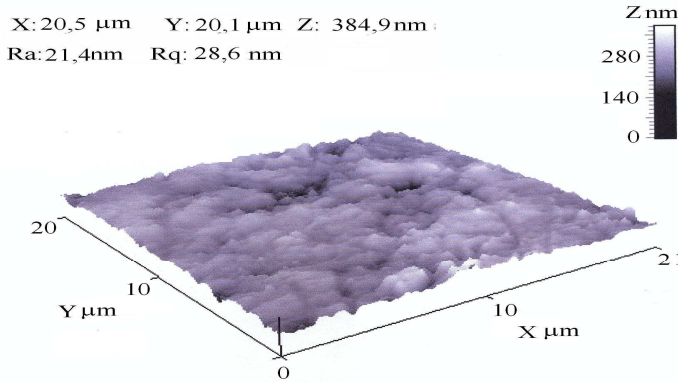


Fig. 5. 3D AFM image of the work surface of the microbearing journal of computer ventilator Kama Flow (Ra = 21.4 nm)

Rys. 5. Widok 3D powierzchni roboczej czopa mikrołożyska w wentylatorze komputerowym Kama Flow (Ra = 21,4 nm) uzyskany na AFM

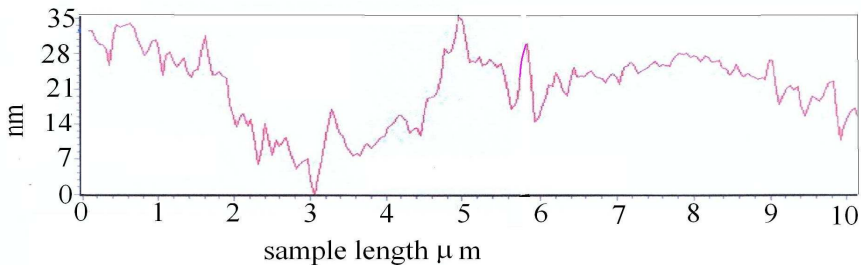


Fig. 6. Profile of the work surface of the journal presenting roughness height in nano-meters versus sample length in micrometers

Fig. 6. Profil powierzchni roboczej czopa pokazujący wysokości chropowatości w nanometrach po długości próbki w mikrometrach

Fig. 6 shows, that the roughness of the journal working surface attain the height of about $20 \cdot 10^{-9}$ m (20 nm). The narrow roughness measurements are about $15 \cdot 10^{-8}$ m (150 nm) wide and 10^{-7} m (100 nm deep).

AFM ROUGHNESS TEST FOR SLEEVE SURFACE

The roughness of the journal working surface is measured in 3D space by the Atomic Force Microscope in the view field $101 \cdot 10^{-7} \text{ m} \times 101 \cdot 10^{-7} \text{ m} \times 384.9 \cdot 10^{-7} \text{ m}$ for calculated parameters: $R_a = 11.9 \text{ nm}$, $R_q = 17.6 \text{ nm}$. The results are presented in **Fig. 7**.

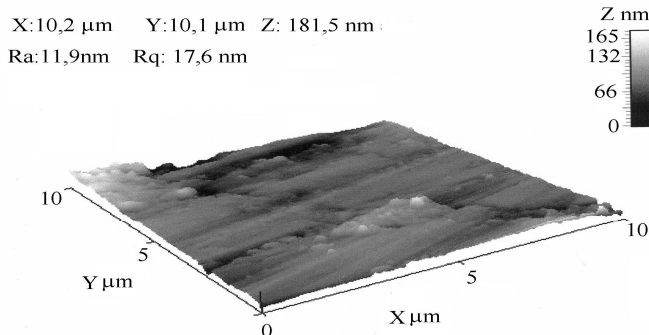


Fig. 7. 3D AFM image of the work surface of the microbearing sleeve of the computer ventilator ($R_a = 21.4 \text{ nm}$)

Rys. 7. Widok 3D powierzchni roboczej panewki mikrołożyska w wentylatorze komputerowym Kama Flow ($R_a = 21,4 \text{ nm}$) uzyskany na AFM

The cross section along the sample presented in **Fig. 7** illustrates the height roughness and the profile of the journal surface in **Fig. 8**. There are no grooves. The material is not damaged. **Fig. 8** shows that the roughness of the sleeve working surface attained the height of about $12 \cdot 10^{-9} \text{ m}$ (12 nm). One visible distance between the tops of roughness is about 10^{-5} m (10 000 nm) wide and $35 \cdot 10^{-9} \text{ m}$ (35 nm) deep.

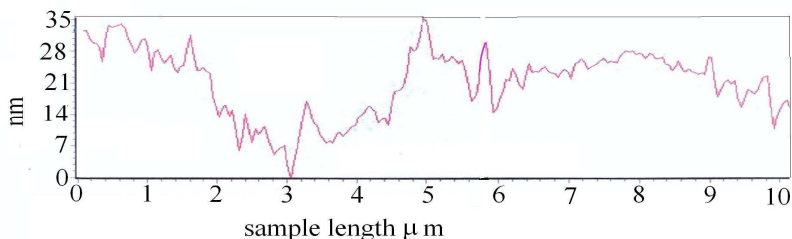


Fig. 8. Profile of the work surface of the sleeve presenting roughness height in nano-meters versus sample length in micrometers

Rys. 8. Profil powierzchni roboczej panewki pokazujący wysokości chropowatości w nanometrach po długości próbki w mikrometrach

GROOVES MEASUREMENTS OF SLEEVE SURFACE

Now we are going to measure the profiles of the groove's cross sections occurring in sleeve surfaces presented in **Fig. 4**. The macroprofile of the section across the herringbone grooves presented in **Figs. 4a, c** are illustrated in **Fig. 9**. Here is shown that the roughness on the sleeve working surface attain a value of about $2 \cdot 10^{-7}$ m (200 nm) and the herringbone groove is $3 \cdot 10^{-6}$ m (3000 nm) deep and $5 \cdot 10^{-5}$ m (50 000 nm) wide. The boundary slopes of the groove are very steep. Microprofile AFM of the section across the longitudinal grooves presented in **Fig. 4b** are illustrated in **Fig. 10**. It is easy to see in **Fig. 8** that the longitudinal groove is about $6 \cdot 10^{-7}$ m (600 nm) deep and from 10^{-4} m (10 000) to $2 \cdot 10^{-4}$ m (20 000 nm) in width. The groove has approximately triangular in shape. Lateral slopes are less steep than in the herringbone groove.

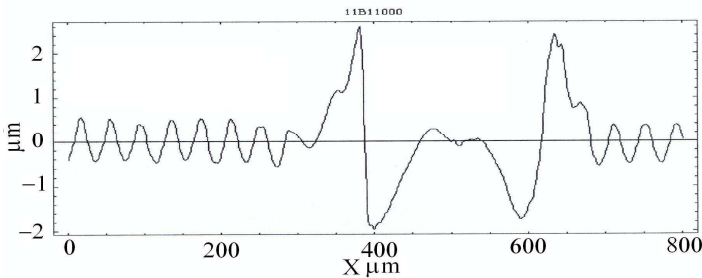


Fig. 9. Macro profile of sleeve work surface in across herring-bone groove depth in micrometers versus length direction of the section in micrometers

Rys. 9. Mikroprofil powierzchni roboczej panewki w poprzek rowka w jodełkę o głębokości w mikrometrach po kierunku długości przekroju w mikrometrach

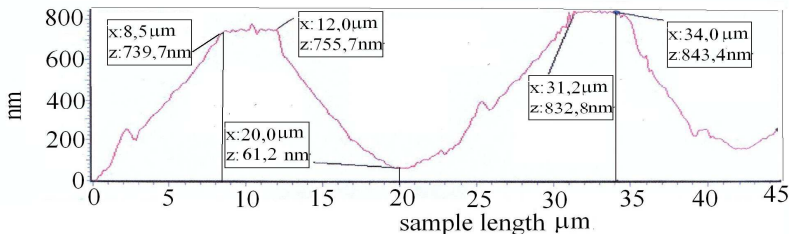


Fig. 10. Micro profile AFM of sleeve work surface across longitudinal groove depth (μm) versus length direction of the section in micrometers

Rys. 10. Mikroprofile powierzchni roboczej panewki w poprzek głębokości (μm) wzdłużnego rowka w kierunku długości przekroju w mikrometrach uzyskane na AFM

MICROHARDNESS AND MODULUS OF ELASTICITY STUDIES

Vickers hardness test was performed by indentation of a diamond pyramid into the sample material with a load of 100 grams. Average values of Vickers Micro-hardness are 7810 MPa for the journal and 2310 MPa for the sleeve. The standard technique MICROHARDNESS TESTER PMT-3M (LOMO-Russia) was utilised for the indentation. The Moduli of Elasticity measurements were performed utilising AFM by indentation of a diamond probe with a 10^{-7} m (100 nm) radius of tip. The reference material for measurements was diamond.

CONCLUSIONS

The measurements performed in the micro and nano scale of the journal with (3mm diameter) and sleeve surfaces occurring in the computer ventilator Kama Flow SP0825FDB12H 80mm, enable one to derive the proper model of analytical and numerical calculations and the development of real exploitation parameters for microbearing lubrication occurring in computer ventilators.

Acknowledgement

Authors thank for the financial help of Polish Ministerial Grant 3475/B/T02/2009/36 in years 2009-2012

REFERENCES

1. Jang, G.H., Seo, C.H., Ho Scong Lee: Finite element model analysis of an HDD considering the flexibility of spinning disc-spindle, head-suspension-actuator and supporting structure, *Microsystem Technologies*, 2007, 13, pp. 837–847.
2. Wierzcholski K., Miszczak A.: Adhesion Influence on the Oil Velocity and Friction Forces in Hyperbolic Microbearing Gap. *Journal of Kones Power-train and Transport*, Warsaw 2010, Vol.17, No.3, pp. 483–489.
3. Wierzcholski K., Miszczak A.: Adhesion Influence on the Oil Velocity and Friction Forces in Cylindrical Microbearing Gap. *Scientific Problems of Machines Operation and Maintenance*, Polish Academy of Sciences (Zagadnienia Eksploatacji Maszyn Kwartalnik PAN), 2010, z.1 (161), Vol. 45, pp. 71–79.

4. Chizhik S., Khudoley A., Kuznetsova T., Wierzcholski K., Miszczak A.: Micro and Nanoscale Wear Studies of HDD Slide Bearings By Atomic Force Microscopy. Proceedings of Methodological Aspects of Scanning Probe Microscopy, Heat and Mass Transfer Institute of NAS, Minsk 2010, pp. 247–252.
5. Liu L.X., Spakovszky Z.S.: Effects of Bearing Stiffness Anisotropy on Hydrostatic Micro gas Journal Bearing Dynamic Behavior, Journal of Engineering for Gas Turbines and Power, ASME, Jan. 2007, Vol. 129, pp. 177–184.
6. Yong-Bok Lee, Hyun-Duck Kwak, Chang-Ho-Kim, Nam-Soo Lee: Numerical prediction of slip flow effect on gas-lubricated journal bearing for MEMS/MST- based micro-rotating machinery. Tribology International, 38, 2005, pp. 89–96.

Recenzent:
Jarosław SEP

Streszczenie

W niniejszej pracy została przedstawiona analiza pomiarów dwóch nowych, niezużytych współpracujących powierzchni mikrołożyska występujących w wentylatorze komputerowym Kama Flow SP0825FDB12H 0,080 m. Powierzchnie te zasadniczo różnią się od powierzchni mikrołożysk HDD. Dlatego też są oddzielnie rozpatrywane. Opracowane pomiary zawierają: obrazy skaningowego elektronowego mikroskopu (SEM), obrazy powierzchni roboczych czopa i panewki, testy AFM powierzchni roboczych czopa i panewki w trzech wymiarach, a także profile ich przekrojów poprzecznych, badania wartości mikrotwardości Vickersa uzyskane na testerze PMT-3M LOMO-Russia dla materiału czopa i panewki. Pomiary powierzchni czopa wykazują chropowatości o wysokości około 80 nm. Powierzchnia panewki zawiera makro- i mikroprofile przekrojów poprzecznych rowków wzdłużnych o głębokości $6 \cdot 10^{-7}$ m (600 nm) i profilu trójkątnym oraz rowki na kształt jodełki o głębokości około 2000 nanometrów o stromych stokach. Takie pomiary umożliwią opracowanie prawidłowych modeli hydrodynamicznej teorii smarowania mikrołożysk w wentylatorach komputerowych o współpracujących powierzchniach z wyciętymi nanorówkami i nanożeberkami uniemożliwiającymi powstawanie niestabilnych wirów i zwiększającymi nośność łożyska. Pomiary zostały wykonane z użyciem mikroskopu sił atomowych.

